PAPER Special Section on Multi-carrier Signal Processing Techniques for Next Generation Mobile Communications

Frequency-Domain Pre-Equalization Transmit Diversity for MC-CDMA Uplink Transmission

Hiromichi TOMEBA[†a)], **Shinsuke TAKAOKA**[†], ***Student Members***, ***and*** **Fumiyuki ADACHI**[†], ***Member***

SUMMARY Recently, multi-carrier code division multiple access (MC-CDMA) has been attracting much attention for the broadband wireless access in the next generation mobile communications systems. In the case of uplink transmissions, the orthogonality among users' signals is lost since each user's signal goes through different fading channel and hence, multi-access interference (MAI) is produced, thereby significantly degrading the transmission performance compared to the downlink case. The use of frequency-domain equalization at the receiver cannot sufficiently suppress the MAI. In this paper, we propose frequency-domain pre-equalization transmit diversity (FPTD), which employs pre-equalization using multiple transmit antennas with transmit power constraint, in order to transform a frequency-selective channel seen at a receiver close to the frequency-nonselective channel. We theoretically analyze the bit error rate (BER) performance achievable with the proposed FPTD and the analysis is confirmed by computer simulation.

key words: *pre-equalization, transmit diversity, MC-CDMA, frequency-domain equalization, frequency-selective channel*

1. Introduction

High speed and high quality data transmissions are required for the next generation mobile communication systems. However, mobile channel is composed of many propagation paths with different time delays, producing severe frequency-selective fading channel, and therefore, the transmission performance degrades due to severe intersymbol inference (ISI) [1]. Recently, multi-carrier code division multiple access (MC-CDMA), which uses a number of lower rate subcarriers to reduce the ISI resulting from frequency-selective channel, has been attracting much attention [2], [3]. Multiple access capability is attained by frequency-domain spreading using user-specific orthogonal spreading codes. In the case of downlink, a good bit error rate (BER) performance can be achieved by using frequency-domain equalization (FDE) at the receiver [4]. However, in the case of uplink, each user's signal goes through different fading channel, and the orthogonality among users is lost, resulting in multi-access interference (MAI), and hence, the BER performance degrades [3]. The BER performance cannot be sufficiently improved by using only the frequency-domain equalization at the receiver.

The multi-user detection and the interference cancellation can be employed at a receiver to suppress the MAI and thus, improve the MC-CDMA uplink transmission performance and they have been researched vigorously [5], [6]. However, recently, frequency-domain pre-equalization at a transmitter has been attracting much attention [7]–[9]. In [7]–[9], a single antenna is used and frequency-domain pre-equalization similar to the FDE reception is applied at a transmitter. Unlike the previous works [7]–[9], in this paper, we apply the transmit diversity technique [10]–[13] to each subcarrier of MC-CDMA signal and propose a frequency-domain pre-equalization transmit diversity (FPTD) (i.e, subcarrier-by-subcarrier pre-equalization is implemented by transmit antenna diversity). By applying transmit diversity technique on each subcarrier, a frequency-selective channel can be transformed into a close-to-non-frequency selective channel, and thus, the MAI can be effectively suppressed. In MC-CDMA uplink with FPTD, orthogonal spreading codes are assigned to different users unlike the conventional MC-CDMA uplink transmission. However, if the received signals at a base station are asynchronous, orthogonality among different users is lost even if the channel is transformed into a close-to-non-frequency selective channel by FPTD and hence, the BER performance significantly degrades; therefore, accurate transmit timing control is necessary. In this paper, we also evaluate the impact of timing control error.

For performing FPTD, the knowledge of the uplink fading channel is required. The uplink fading channel can be estimated using the downlink channel in the case of time division duplex (TDD), which uses the same carrier frequency for both uplink and downlink channels. TDD has the flexibility in assigning the limited channel resources to uplink and downlink. Another advantage of TDD is that channel reciprocity (fading is highly correlated between the uplink and downlink as the same carrier frequency is used for both uplink and downlink) facilitates adaptive communication techniques. Therefore, TDD is considered as a promising duplex technique in the next generation mobile communication systems [14].

In this paper, we assume MC-CDMA using TDD and evaluate the uplink BER performance achievable with the proposed FPTD. The complexity of the mobile terminals increases with the use of FPTD. In this paper, we show that at the cost of increasing complexity of the mobile terminals, the use of FPTD can significantly improve the MC-CDMA uplink transmission performance in a multi-user environment.

The remainder of this paper is organized as follows.

Manuscript received May 28, 2004.
Manuscript revised August 20, 2004.

[†]The authors are with the Department of Electrical and Communication Engineering, Graduate School of Engineering, Tohoku University, Sendai-shi, 980-8579 Japan.
a) E-mail: tomeba@mobile.ecei.tohoku.ac.jp

Sect. 2 describes the proposed FPTD for the MC-CDMA uplink transmission. Then, the BER performance achievable with the proposed FPTD is theoretically analyzed in Sect. 3. In the theoretical analysis, the conditional BER is derived for a given set of channel gains to compute the theoretical average BER. In Sect. 4, the theoretical average BER performance is numerically evaluated by Monte-Carlo numerical computation method using the derived expression for the conditional BER and confirmed by computer simulation. Sect. 5 offers some conclusions.

2. Proposed FPTD for MC-CDMA Uplink Transmission

Figure 1 illustrates the transmitter and receiver structure employing the proposed FPTD for the jth user. At the transmitter, a sequence of modulated data symbols to be transmitted is spread in time-domain by an orthogonal spreading code with the spreading factor SF to obtain the chip sequence (we assume that orthogonal spreading codes are used unlike the conventional uplink transmission of MC-CDMA, where pseudo-random spreading codes are used by different users). After serial-to-parallel (S/P) conversion, the chip sequence is converted into N_c (N_c is the number of subcarriers) parallel streams, each of which is multiplied by N_t pre-equalization weights, where N_t represents the number of transmit antennas. Then, N_c-point inverse fast Fourier transform (IFFT) is applied to generate the pre-equalized MC-CDMA signals to be transmitted from N_t transmit antennas after insertion of the guard interval (GI). N_t pre-equalized MC-CDMA signals transmitted over a frequency-selective channel are superimposed and received at a base station receiver. At the base station receiver, after removal of GI from the received MC-CDMA signal, N_c-point FFT is applied to decompose it into the N_c subcarrier components. After parallel-to-serial (P/S) conversion, despreading is carried out, followed by data demodulation. Note that no FDE is required at the base station receiver, while it is needed at the mobile terminal receiver for the downlink signal reception.

In what follows, without loss of generality, we assume a transmission of N_c/SF data symbols $\{d_j(m);\ m = 0 \sim N_c/SF - 1\}$ over one MC-CDMA signaling interval.

2.1 Pre-Equalization

Using the pre-equalization weight vector $\boldsymbol{w}_j(k) = [w_j(0,k), w_j(1,k), \ldots, w_j(N_t-1,k)]^T$, the transmit signal vector of the jth user at the kth subcarrier can be expressed as

$$\begin{aligned}\boldsymbol{s}_j(k) &= [s_j(0,k), s_j(1,k), \ldots, s_j(N_t-1,k)]^T \\ &= \sqrt{\frac{2S}{SF}}\boldsymbol{w}_j(k)c_j(k \bmod SF)d_j(m) \end{aligned} \quad (1)$$

with

$$\left\|\boldsymbol{w}_j(k)\right\|^2 = 1, \quad (2)$$

where S, $c_j(k)$, and $d_j(m)$ denote the total transmit signal power, the kth chip of the orthogonal spreading code with spreading factor SF with $|c_j(k)|$=1, and the mth data-modulated symbol, respectively, and $\|\cdot\|$ represents the vector norm operation. We propose to use subcarrier-by-subcarrier pre-equalization schemes based on the well known diversity combining schemes [1], using maximal ratio combining (MRC), equal gain combining (EGC), and selection combining (SC). Furthermore, a new pre-equalization scheme is proposed that is based on what we call the controlled equalization combining (CEC). In CEC, a threshold is introduced; EGC is used if the equivalent transmit channel gain after pre-equalization is above the threshold and MRC is used otherwise, in order to more effectively suppress the variations in the equivalent channel gain than MRC, EGC and SC. The nth element $w_j(n,k)$ of $\boldsymbol{w}_j(k)$ is given by

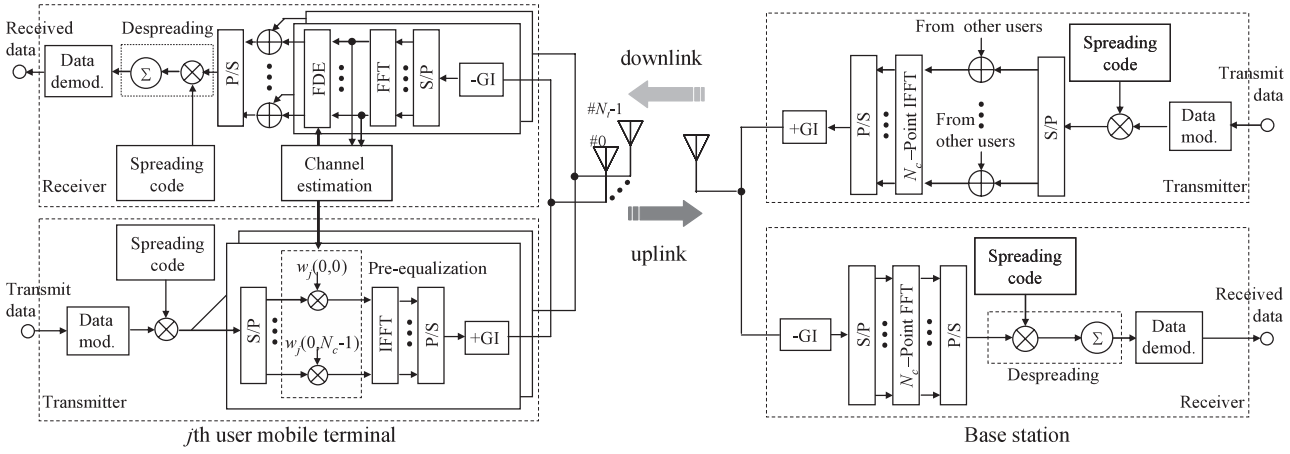

Fig. 1 Transmitter and receiver structure of MC-CDMA using FPTD.

$$w_j(n,k) = \begin{cases} \dfrac{H_j^*(n,k)}{\sqrt{\sum_{n=0}^{N_t-1}|H(n,k)|^2}}, & \text{MRC} \\ \dfrac{1}{\sqrt{N_t}}\dfrac{H_j^*(n,k)}{\left|H_j(n,k)\right|}, & \text{EGC} \\ \begin{cases} \dfrac{H_j^*(n,k)}{\left|H_j(n,k)\right|}, \text{if } \left|H_j(n,k)\right| = \arg\max\limits_{n'}\{|H_j(n',k)|\} \\ 0, \quad \text{otherwise,} \end{cases} & \text{SC} \\ \begin{cases} \dfrac{H_j^*(n,k)}{\sqrt{\sum_{n=0}^{N_t-1}|H(n,k)|^2}}, & \text{if } \left|\tilde{H}_{MRC,j}(k)\right| < \gamma_0 \\ \dfrac{1}{\sqrt{N_t}}\dfrac{H_j^*(n,k)}{\left|H_j(n,k)\right|}, & \text{otherwise,} \end{cases} & \text{CEC} \end{cases} \tag{3}$$

where, $H_j(n,k)$ represents the nth element of the channel gain vector of $\boldsymbol{H}_j(k) = [H_j(0,k), H_j(1,k), \ldots, H_j(N_t-1,k)]^T$ of the jth user and $\tilde{H}_{MRC,j}(k)$ is the equivalent channel gain observed at the receiver, given by

$$\tilde{H}_{MRC,j}(k) = \boldsymbol{H}_j^T(k)\boldsymbol{w}_{MRC,j}(k). \tag{4}$$

It can be understood from Eq. (3) that since the complex conjugation of the channel gain is used in the pre-equalization weight, all users' signals are received in phase and hence the MAI is reduced.

MRC pre-equalization maximizes the received instantaneous signal-to-noise power ratio (SNR) at the mobile receiver, while EGC pre-equalization equalizes the phase only. In SC, one of the N_t transmit antennas providing the strongest channel gain is selected to transmit each subcarrier after phase equalization. The difference of our SC pre-equalization from a transmit antenna diversity scheme presented in Ref. [13] is that in our proposed scheme, phase equalization is used in order to make all subcarrier components arrive at the receiver in phase. CEC acts as EGC (or MRC) when the MRC equivalent channel gain is larger (or smaller) than the prescribed threshold value γ_0. By doing so, the frequency-selectivity of the pre-equalized channel seen at the receiver can be suppressed well compared with MRC and EGC pre-equalizations.

Applying N_c-point IFFT to $\boldsymbol{s}_j(k)$, the pre-equalized MC-CDMA signal vector is obtained as

$$\begin{aligned} \tilde{\boldsymbol{s}}_j(t) &= \sum_{k=0}^{N_c-1} \boldsymbol{s}_j(k)\exp(j2\pi tk/N_c) \\ &= [\tilde{s}_j(0,t), \tilde{s}_j(1,t), \ldots, \tilde{s}_j(N_t-1,t)]^T, \\ &\quad \text{for } t = 0 \sim N_c - 1. \end{aligned} \tag{5}$$

After insertion of the GI, the pre-equalized MC-CDMA signal vector is transmitted using N_t transmit antennas.

2.2 Fading Channel

The fading channel composed of L independent propagation paths is assumed. The time delay of the lth path is assumed to be lT_c, with T_c representing the FFT/IFFT sampling period. Using path gain vector $\boldsymbol{h}_{j,l} = [h_{j,l,0}, h_{j,l,1}, \ldots, h_{j,l,Nt-1}]^T$ of the lth path for the jth user, the channel gain vector $\boldsymbol{H}_j(k)$ can be expressed as

$$\boldsymbol{H}_j(k) = \left[\boldsymbol{h}_{j,0}, \ldots, \boldsymbol{h}_{j,l}, \ldots, \boldsymbol{h}_{j,L-1}\right] \begin{bmatrix} 1 \\ \vdots \\ \exp(-j2\pi kl/N_c) \\ \vdots \\ \exp(-j2\pi k(L-1)/N_c) \end{bmatrix}. \tag{6}$$

2.3 Received Signal and Despreading

Transmit timing control is assumed such that the time delays of all paths of all users are within the GI. The received signal is the superimposition of MC-CDMA signals transmitted from U different users and can be expressed as

$$r(t) = \sum_{j=0}^{U-1}\sum_{l=0}^{L-1} \boldsymbol{h}_{j,l}^T \tilde{\boldsymbol{s}}_j(t-l) + n(t), \tag{7}$$

where $n(t)$ represents the complex-valued zero mean additive white Gaussian noise (AWGN). After removal of GI from the superimposed received MC-CDMA signal, N_c-point FFT is applied to decompose it into the N_c subcarrier components. The kth subcarrier component $R(k)$ is represented as

$$\begin{aligned} R(k) &= \sum_{j=0}^{U-1} \boldsymbol{H}_j^T(k)\boldsymbol{s}_j(k) + n(k) \\ &= \sqrt{\frac{2S}{SF}}\sum_{j=0}^{U-1} \tilde{H}_j(k)c_j(k \bmod SF)d_j(m) + n(k), \end{aligned} \tag{8}$$

where

$$\tilde{H}_j(k) = \boldsymbol{H}_j^T(k)\boldsymbol{w}_j(k) \tag{9}$$

is the equivalent channel gain associated with the jth user at the kth subcarrier. The soft decision value $\hat{d}_j(m)$, $m = 0 \sim N_c/SF - 1$, for the mth data-modulated symbol of the jth user is obtained by despreading as

$$\hat{d}_j(m) = \frac{1}{SF}\sum_{k=mSF}^{(m+1)SF-1} R(k)c_j^*(k \bmod SF). \tag{10}$$

Substituting Eq. (8) into Eq. (10), we have

$$\hat{d}_j(m) = \sqrt{\frac{2S}{SF}}\left(\frac{1}{SF}\sum_{k=mSF}^{(m+1)SF-1}\tilde{H}_j(k)\right)d_j(m) + \mu_{MAI} + \mu_{AWGN}, \tag{11}$$

where the first term represents the desired signal component and the second and third terms denote the MAI component and the noise component due to the AWGN, respectively, and are given by

$$\begin{cases} \mu_{MAI} = \dfrac{1}{SF}\sqrt{\dfrac{2S}{SF}}\displaystyle\sum_{k=mSF}^{(m+1)SF-1}\sum_{\substack{u=0\\u\neq j}}^{U-1}\left\{\begin{array}{l}\tilde{H}_u(k)c_u(k \bmod SF)\\ \times c_j^*(k \bmod SF)d_u(m)\end{array}\right\} \\ \mu_{AWGN} = \dfrac{1}{SF}\displaystyle\sum_{k=mSF}^{(m+1)SF-1} n(k)c_j^*(k \bmod SF). \end{cases} \tag{12}$$

3. Theoretical Analysis of Average BER

It can be understood from Eq. (11) that the despreader output $\hat{d}(m)$ is a complex-valued random variable with mean $\sqrt{\frac{2S}{SF}}\left(\frac{1}{SF}\sum_{k=mSF}^{(m+1)SF-1}\tilde{H}_j(k)\right)d_j(m)$. Approximating μ_{MAI} as a zero-mean complex-valued Gaussian process, the sum of μ_{MAI} and μ_{AWGN} can be treated as a new zero-mean complex-valued Gaussian noise μ. The variance of μ is the sum of those of μ_{MAI} and μ_{AWGN}:

$$2\sigma_\mu^2 = E[|\mu|^2] = 2\sigma_{\mu_{MAI}}^2 + 2\sigma_{\mu_{noise}}^2, \tag{13}$$

where, from Appendix,

$$\begin{cases} \sigma_{MAI}^2 = \dfrac{1}{2}E\left[\,|\mu_{MAI}|^2\right] = \dfrac{S}{SF^2}\displaystyle\sum_{\substack{u=0\\u\neq j}}^{U-1} \\ \quad\left(\dfrac{1}{SF}\displaystyle\sum_{k=mSF}^{(m+1)SF-1}\left|\tilde{H}_u(k)\right|^2 - \left|\dfrac{1}{SF}\displaystyle\sum_{k=mSF}^{(m+1)SF-1}\tilde{H}_u(k)\right|^2\right) \\ \sigma_{AWGN}^2 = \dfrac{1}{2}E\left[\,|\mu_{AWGN}|^2\right] = \dfrac{1}{SF}\dfrac{N_0}{N_cT_c} \end{cases} \tag{14}$$

for a given set of $\{\boldsymbol{H}_j(k);\ j = 0 \sim U-1 \text{ and } k = 0 \sim N_c-1\}$, where N_0 is the single sided AWGN power spectrum density. Therefore, we have

$$\sigma_\mu^2 = \frac{1}{SF}\left[\frac{N_0}{N_cT_c} + \frac{S}{SF}\sum_{\substack{u=0\\u\neq j}}^{U-1}\left(\frac{1}{SF}\sum_{k=mSF}^{(m+1)SF-1}\left|\tilde{H}_u(k)\right|^2 - \left|\frac{1}{SF}\sum_{k=mSF}^{(m+1)SF-1}\tilde{H}_u(k)\right|^2\right)\right]. \tag{15}$$

We assume quaternary phase shift keying (QPSK) data-modulation and all "1" transmission without loss of generality. Since the MAI can be assumed to be circularly symmetric, the conditional BER for a given set of $\{\boldsymbol{H}_j(k);\ j = 0 \sim U-1 \text{ and } k = 0 \sim N_c-1\}$ can be given by

$$p_b\left(\frac{E_s}{N_0}, \{\boldsymbol{H}_j(k)\}\right) = \frac{1}{2}erfc\left[\sqrt{\frac{1}{4}\gamma\left(\frac{E_s}{N_0}, \{\boldsymbol{H}_j(k)\}\right)}\right], \tag{16}$$

where E_s $(=SN_cT_c)$ is the transmit symbol energy, $erfc[x] = (2/\sqrt{\pi})\int_x^\infty \exp(-t^2)dt$ is the complementary error function and $\gamma(E_s/N_0, \{\boldsymbol{H}_j(k)\})$ is the conditional signal-to-interference plus noise power ratio (SINR), given by

$$\begin{aligned}\gamma\left(\frac{E_s}{N_0}, \{\boldsymbol{H}_j(k)\}\right) &= \frac{\dfrac{2S}{SF}\left|\dfrac{1}{SF}\displaystyle\sum_{k=mSF}^{(m+1)SF-1}\tilde{H}_j(k)\right|^2}{\sigma_\mu^2} \\ &= \frac{2\dfrac{E_s}{N_0}\left|\dfrac{1}{SF}\displaystyle\sum_{k=mSF}^{(m+1)SF-1}\tilde{H}_j(k)\right|^2}{1 + \dfrac{1}{SF}\dfrac{E_s}{N_0}\displaystyle\sum_{\substack{u=0\\u\neq j}}^{U-1}\left(\dfrac{1}{SF}\displaystyle\sum_{k=mSF}^{(m+1)SF-1}\left|\tilde{H}_u(k)\right|^2 - \left|\dfrac{1}{SF}\displaystyle\sum_{k=mSF}^{(m+1)SF-1}\tilde{H}_u(k)\right|^2\right)}.\end{aligned} \tag{17}$$

The theoretical average BER can be numerically evaluated by averaging Eq. (16) over $\{\boldsymbol{H}_j(k);\ j = 0 \sim U-1 \text{ and } k = 0 \sim N_c-1\}$:

$$P_b\left(\frac{E_s}{N_0}\right) = \int\cdots\int\frac{1}{2}erfc\left[\sqrt{\frac{1}{4}\gamma\left(\frac{E_s}{N_0}, \{\boldsymbol{H}_j(k)\}\right)}\right] \times p(\{\boldsymbol{H}_j(k)\})\prod_{j,k}d\boldsymbol{H}_j(k), \tag{18}$$

where $p(\{\boldsymbol{H}_j(k)\})$ is the joint probability density function (pdf) of $\{\boldsymbol{H}_j(k);\ j = 0 \sim U-1 \text{ and } k = 0 \sim N_c-1\}$.

4. Numerical and Simulation Results

4.1 Numerical and Simulation Conditions

Table 1 summarizes the numerical and simulation conditions. QPSK data-modulation is considered as assumed in

Table 1 Numerical and simulation conditions.

Data modulation			QPSK
MC-CDMA	No. of subcarriers		N_c=256
	Guard interval		N_g=32
FPTD	Pre-equalization weights		MRC, EGC, SC, CEC
	No. of transmit antennas		N_t=1, 2, 4
	Spreading factor		SF=64
Channel model	No. of paths		L=16
	Power delay profile		Exponential
		Decay factor	α=0, 4, 8, 16dB
		Time delays	$\tau_l = lT_c$, l=0~L-1
	Normalized maximum Doppler frequency		f_DT=0.001 ($T=(N_s+N_g)T_c$)
Channel estimation			Ideal

Sect. 3. As for the fading channel, a FFT/IFFT sample-spaced L=16-path frequency-selective Rayleigh fading channel having an exponential power delay profile with decay factor α is assumed.

The numerical evaluation of the theoretical average BER performance is done by Monte-Carlo numerical computation method as follows. The set of path gain vector $\{\boldsymbol{h}_{j,l}; j = 0 \sim U-1$ and $l = 0 \sim L-1\}$ is generated for obtaining $\{\boldsymbol{H}_j(k); j = 0 \sim U-1$ and $k = 0 \sim N_c-1\}$ using Eq. (6) and then $\{\boldsymbol{w}_j(k); j = 0 \sim U-1$ and $k = 0 \sim N_c-1\}$ is computed using Eq. (3). The conditional BER for the given transmit E_s/N_0 and $\boldsymbol{H}_j(k)$ is computed using Eq. (16). This is repeated sufficient number of times to obtain the theoretical average BER of Eq. (18).

The BER performance is also evaluated by computer simulation. The computer simulation is carried out as follows. At the transmitter, QPSK data-modulated sequence is generated and spread by an orthogonal spreading code. After L=16-path Rayleigh fading channel is generated, the channel gain vector $\boldsymbol{H}_j(k)$ is computed using Eq. (6) and the pre-equalization weight vector $\boldsymbol{w}_j(k)$ is computed using Eq. (3). Subcarrier components to be transmitted form N_t antennas are pre-equalized by using the pre-equalization weight vector $\boldsymbol{w}_j(k)$. Then, the pre-equalized MC-CDMA signal is generated by performing IFFT (see Eq. (5)) and insertion of GI. At the receiver, the received MC-CDMA signal is generated according to Eq. (7). After GI removal, FFT is carried out to get the frequency-domain signal sequence and then, despreading is carried out to obtain the decision variables for QPSK data-demodulation. The recovered QPSK symbol sequence is compared with the transmitted symbol sequence to measure the number of bit errors. The above transmission and reception procedure is repeated sufficient times to compute the average BER.

4.2 Equivalent Channel Gain with FPTD

How the FPTD transforms the channel closer to the frequency non-selective channel is discussed. Figure 2 shows a one-shot observation of the equivalent channel gain $\tilde{H}(k)$ observed at the base station receiver when FPTD using CEC pre-equalization weight is used. Without pre-equalization, large variations in $\tilde{H}(k)$ are seen. However, as the number N_t of transmit antennas increases, variations in $\tilde{H}(k)$ are reduced and the resultant channel approaches the frequency non-selective channel. Hence, the destruction in orthogonality is reduced, resulting in less MAI.

4.3 Comparison of FPTD Using CEC, MRC, EGC and SC Pre-Equalization Weights

Figure 3 compares the average BER performances achievable with FPTD using CEC, MRC, EGC and SC pre-equalization weights as a function of the transmit E_b/N_0 (=0.5 $(E_s/N_0)(1 + N_g/N_c)$) when N_t=4. The number U of users is assumed to be 1, 32 and 64 in Figs. 3(a), (b) and (c), respectively. Firstly, we compare the average BER performances achievable with FPTD using MRC, EGC and SC. Irrespective of the number of users, the MRC pre-equalization provides the best BER performance among three pre-equalization techniques since the MRC maximizes the instantaneous SNR while suppressing the variations in $\tilde{H}(k)$. However, it can be seen from Fig. 3 that the BER performance with FPTD using MRC degrades as U increases. When U=64, the BER floor of around $BER = 10^{-4}$ is observed since the MAI cannot be sufficiently suppressed by using MRC pre-equalization. Next, we compare the average BER performances with FPTD using CEC and MRC pre-equalizations. It can be seen from Fig. 3 that CEC and MRC provide identical BER performance for the single-user case (U=1); however, CEC provides better BER performance than MRC when U=32 and 64. The reason for this is explained below.

If all the received MC-CDMA signals transmitted from different users are synchronous, MAI is caused by the residual variations in the equivalent channel gain. MAI is proportional to the variance $\sigma^2_{\tilde{H}}$ of the equivalent channel gain $\tilde{H}_u(k)$ (see Eq. (14)), where

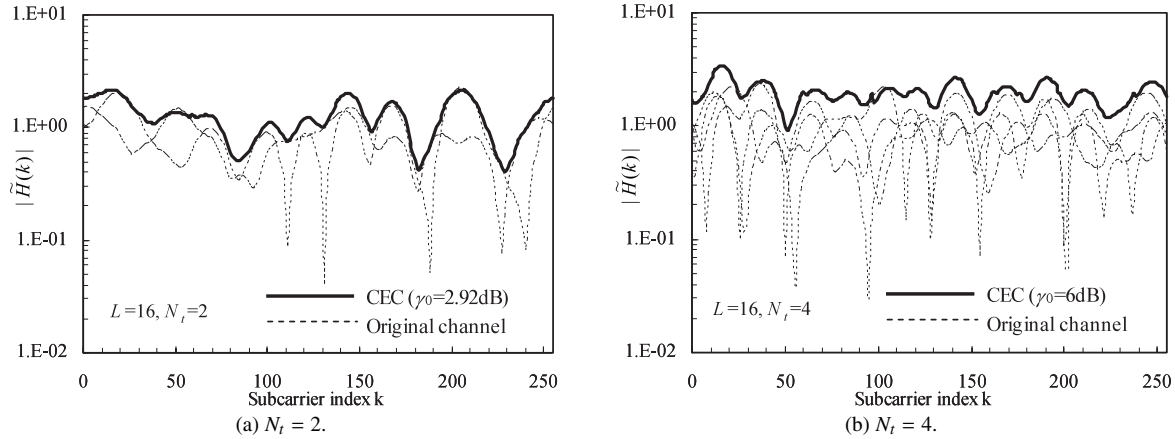

(a) N_t = 2. (b) N_t = 4.

Fig. 2 Equivalent channel transfer function with FPTD.

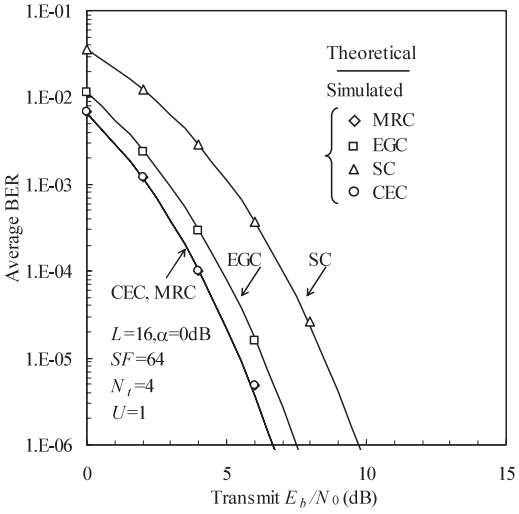

(a) $U = 1$.

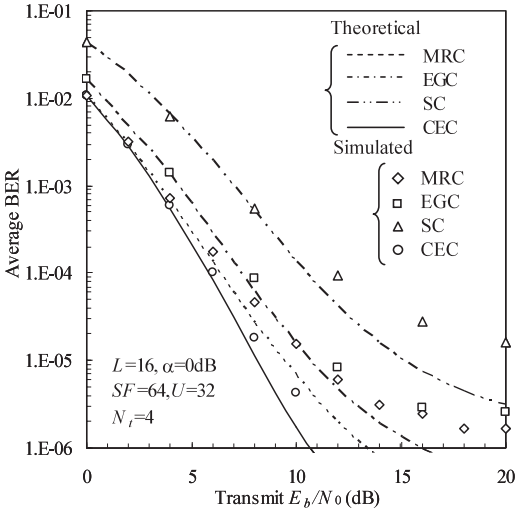

(b) $U = 32$.

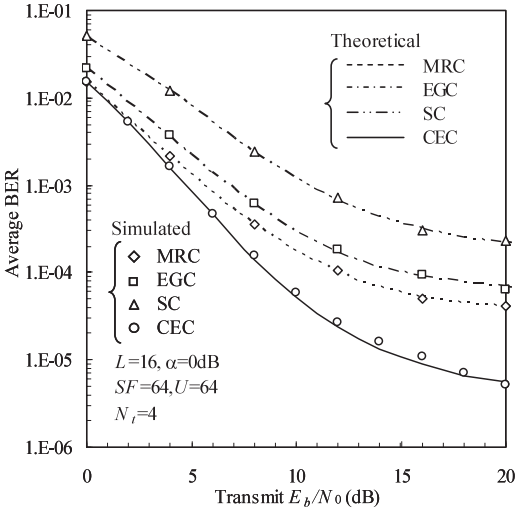

(c) $U = 64$.

Fig. 3 Average BER performance of FPTD using CEC, MRC, EGC and SC pre-equalizations.

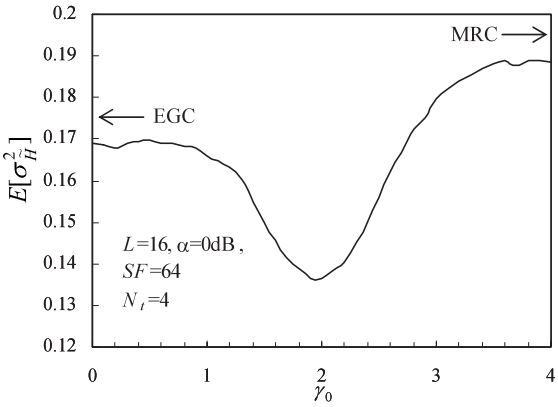

Fig. 4 Dependency of MAI on γ_0.

$$\sigma^2_{\tilde{H}} = \frac{1}{SF}\sum_{k=mSF}^{(m+1)SF-1}\left|\tilde{H}_u(k) - \frac{1}{SF}\sum_{k=mSF}^{(m+1)SF-1}\tilde{H}_u(k)\right|^2$$
$$= \frac{1}{SF}\sum_{k=mSF}^{(m+1)SF-1}\left|\tilde{H}_u(k)\right|^2 - \left|\frac{1}{SF}\sum_{k=mSF}^{(m+1)SF-1}\tilde{H}_u(k)\right|^2. \quad (19)$$

In CEC pre-equalization (see Eq. (3)), the equivalent channel gain $\tilde{H}_{MRC,u}(k)$ obtained by MRC is compared with the threshold γ_0 at each subcarrier. When $\tilde{H}_{MRC,u}(k) > \gamma_0$, EGC weight is used in order to avoid the excessive enhancement in the equivalent channel gain. Otherwise, MRC weight is used for enhancing the equivalent channel gain. By doing so, it is expected that the variations in the equivalent channel gain can be reduced compared to the case when only MRC or EGC is used. Fig. 4 shows the ensemble average of $E[\sigma^2_{\tilde{H}}]$ as a function of γ_0. For comparison, $E[\sigma^2_{\tilde{H}}]$ is also indicated for MRC and EGC in Fig. 4 (note that CEC with $\gamma_0 \to \infty$ (0) corresponds to MRC (EGC)). It can be seen that CEC can reduce the value of $E[\sigma^2_{\tilde{H}}]$ and hence reduces the MAI compared to MRC and EGC, by optimizing the value of γ_0. The optimum γ_0 is seen to be γ_0=2. By using $\gamma_0 = 2$, FPTD using CEC provides better BER performance than MRC and EGC. It is clearly seen in Fig. 5, which plots the average BER performance as a function of the threshold γ_0. Although the optimum value of γ_0 depends on the values of U and E_b/N_0, the use of γ_0=2 provides the best BER performance except for the single-user case (U=1). For the single-user case, the dominant cause for bit errors is the AWGN and hence the optimum value of γ_0 is $\gamma_0 \to \infty$ (MRC) so that the SNR can be maximized. Therefore, in the case of U=1, the BER performance of both CEC-FPTD and MRC-FPTD are the same.

In Fig. 3, the deviations between the theoretical and simulated performances are seen when U=32. The theoretical analysis is based on the Gaussian approximation of the MAI (see Appendix). Performance deviations are due to the fact that the MAI is not well approximated by a Gaussian process. However, when U=64, the MAI approaches a Gaussian process according to the central limit theorem, and thus, the theoretical and simulated results are in a good

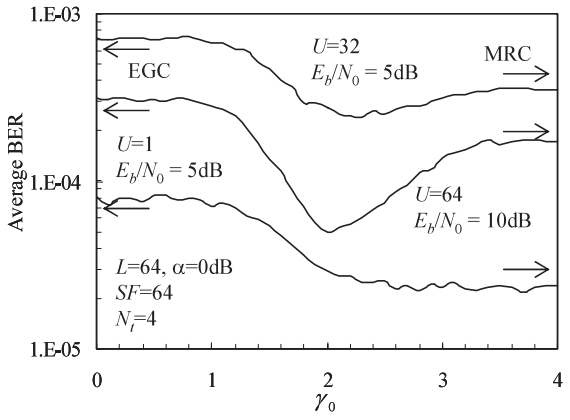

Fig. 5 Effect of γ_0 on BER for FPTD using CEC.

agreement.

4.4 Comparison of CEC-FPTD and MMSE-FDE Reception Combined with Receive Diversity or STTD

Here, we compare the BER performance achievable with FDE reception using single transmit antenna and N receive antennas (N_t=1 and $N_r = N$) and that with CEC-FPTD using N transmit antennas and single receive antenna ($N_t = N$ and N_r=1). For FDE reception, the minimum mean square error (MMSE) weight is used. The MMSE weight using N_r receive antennas for the uplink is given by [15]

$$w_j^{(n)}(k) = \frac{H_j^{(n)*}(k)}{\sum_{n=0}^{N-1}\sum_{j=0}^{U-1}\left|H_j^{(n)}(k)\right|^2 + \left(\frac{E_s/N_0}{SF}\right)^{-1}}, \tag{20}$$

where $H_j^{(n)}(k)$ is the kth subcarrier channel gain between the jth user and the nth receive antenna at a base station. Also, we compare space-time block coded transmit diversity (STTD) [15], [16] with CEC-FPTD both using N-transmit antennas ($N_t = N$).

Figure 6(a) plots the BER performance of the single-user case (U=1) with the number N of antennas as a parameter. The BER performance of N-transmit antenna CEC-FPTD is slightly worse than that of N-receive antenna MMSE-FDE reception. The required E_b/N_0 degradation with CEC-FPTD for obtaining a $BER = 10^{-4}$ is 0.8 dB, 0.4 dB and 0.2 dB when N=1, 2 and 4, respectively. Also, we can see from Fig. 6(a) that CEC-FPTD achieves a better BER performance than STTD. The required E_b/N_0 improvement from STTD is 2.6 dB (5.8 dB) when N=2 (N=4).

Next, we examine CEC-FPTD, MMSE-FDE reception and STTD for the multi-user case (U=64). The simulated BER performances are plotted in Fig. 6(b), where γ_0 is optimized at the transmit E_b/N_0=10 dB. It is seen that although the BER performances with MMSE-FDE reception and STTD are improved by increasing the number N of antennas, high BER floors are observed. This is because MAI cannot be sufficiently suppressed by MMSE-FDE reception and STTD although the desired user's SNR can be

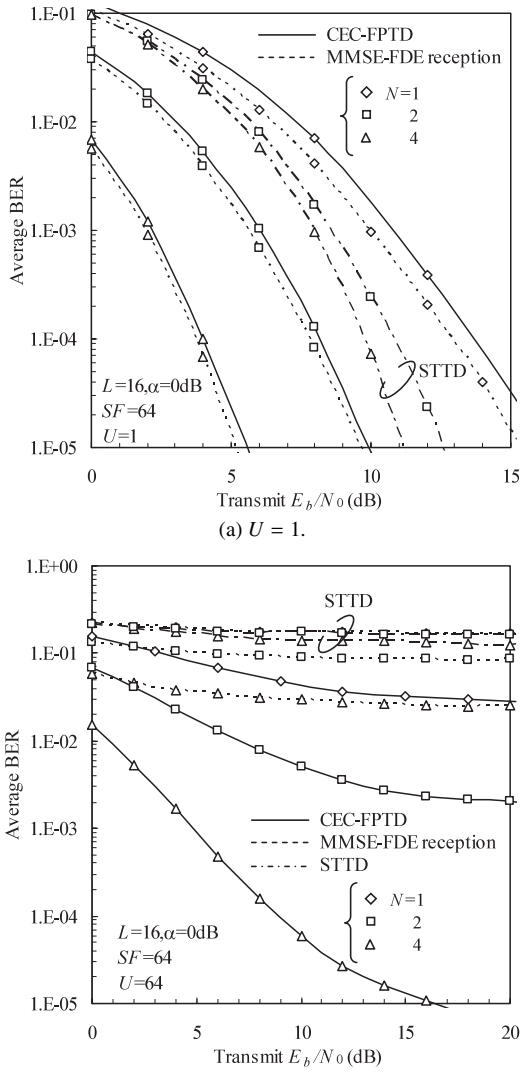

Fig. 6 Performance comparison between CEC-FPTD and MMSE-FDE reception combined with receive diversity or STTD.

improved. On the other hand, CEC-FPTD can transform the each user's transmit channel closer to the frequency non-selective channel while improving the SNR, and therefore, the orthogonality destruction is reduced, resulting in less MAI.

As a sequel, CEC-FPTD can provide significantly better BER performance than MMSE-FDE reception and STTD for the multi-user case, while it is slightly worse for the single-user case. This significant performance superiority of CEC-FPTD is obtained at the cost of increased complexity of mobile terminals.

4.5 Impact of Decay Factor α

So far, we have assumed the decay factor α=0 dB (i.e. a uniform power delay profile). As α increases, the frequency-selectivity becomes weaker and approaches the single-path channel when $\alpha \to \infty$. Since the BER performance depends

on α we evaluate the BER performance with α as a parameter. Figure 7 plots the BER performance of CEC-FPTD as a function of the transmit E_b/N_0 with α as a parameter. When U=1, α=0 dB gives a better BER performance than α=4, 8 and 16 dB due to larger frequency diversity effect. However, when U=64, as α increases the BER performance improves. This is because MAI decreases due to less orthogonality destruction as α increases.

4.6 Impact of Transmit Timing Control Error

So far, we have assumed that all the received MC-CDMA signals transmitted from different users are synchronous by the use of ideal transmit timing control. However, with a practical transmit timing control, there exists the timing error in the received signals, and hence MAI is produced even if each user's equivalent channel can be made closer to the frequency non-selective channel. Hence, accurate transmit timing control is required for FPTD. Here we evaluate, how the transmit timing error affects the achievable BER performance is evaluated. Each user's transmit timing error is assumed to be independent and identically distributed uniformly over $[-T_c\Delta/2, +T_c\Delta/2]$. Figure 8 plots the BER performance of CEC-FPTD as a function of the transmit E_b/N_0 with Δ as a parameter. It is seen that the BER performance is sensitive to Δ and significantly degrades when $\Delta > 1/2$. Therefore, Δ must be maintained less than 1/4.

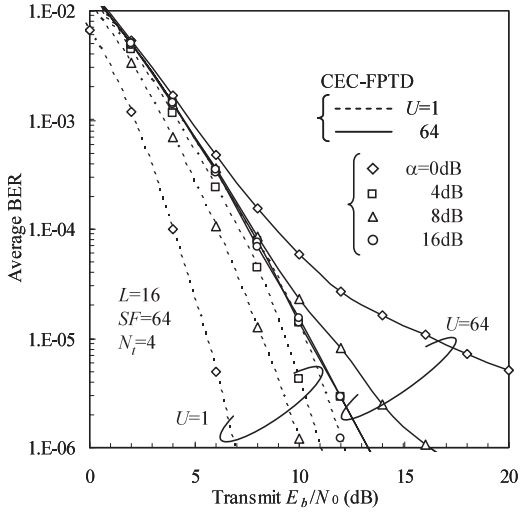

Fig. 7 Impact of the decay factor α.

5. Conclusion

In this paper, frequency-domain pre-equalization transmit diversity (FPTD) for improving the MC-CDMA uplink BER performance was proposed and the average BER performance was theoretically analyzed. The orthogonality among users cannot be restored by the receive frequency-domain equalization (FDE) reception only. However, with FPTD, the equivalent transmit channel of each user can be transformed closer to the frequency non-selective channel and all the subcarriers are in phase for all users, and hence, the orthogonality among different users is restored (unlike the conventional MC-CDMA uplink transmission, orthogonal spreading codes are used by different users), thereby improving the BER performance without applying FDE reception at the receiver. We considered various pre-equalization weights of MRC, EGC, SC and CEC and compared the theoretical BER performances achievable with them to show that CEC provides the best performance. The theoretical results were confirmed by the computer simulation.

The MC-CDMA uplink transmission performance can be significantly improved by using the FPTD at the cost of complexity of mobile terminals. Recently, multi-input multi-output (MIMO) system has been attracting much attention. There is a possibility that the mobile terminal may have more than two transmit antennas in the future. If this happens, the FPTD can be used to significantly improve the

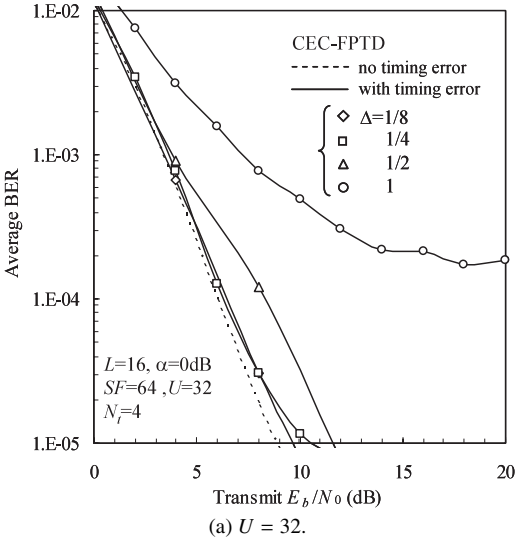

(a) U = 32.

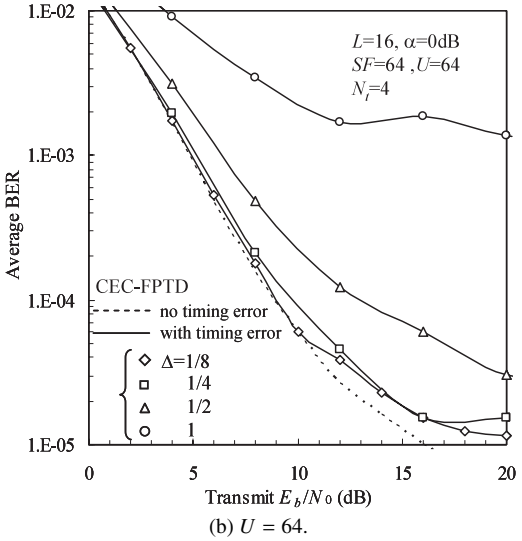

(b) U = 64.

Fig. 8 Impact of the transmit timing error.

MC-CDMA uplink transmission performance. However, FPTD was found to be very sensitive to the transmit timing control error. The timing error must be maintained less than 1/4 samples. Therefore, some transmit timing control technique, as studied for DS-CDMA [17], must be employed. The transmit timing control technique suitable for FPTD is left as an important future study.

References

[1] W.C. Jakes, Jr., ed., Microwave Mobile Communications, Wiley, New York, 1974.
[2] S. Hara and R. Prasad, "Overview of multicarrier CDM," IEEE Commun. Mag., vol.35, no.12, pp.126–133, Dec. 1997.
[3] S. Hara and R. Prasad, "Design and performance of multicarrier CDMA system in frequency-selective Rayleigh fading channels," IEEE Trans. Veh. Technol., vol.48, no.5, pp.1584–1595, Sept. 1999.
[4] T. Sao and F. Adachi, "Comparative study of various frequency equalization techniques for downlink of a wireless OFDM-CDMA systems," IEICE Trans. Commun., vol.E86-B, no.1, pp.352–364, Jan. 2003.
[5] S. Tsumura and S. Hara, "Design and performance of quasi-synchronous multi-carrier CDMA system," Proc. IEEE VTC'01 fall, vol.2, pp.843–847, Oct. 2001.
[6] M.S. Akther, J. Asenstorger, P.D. Alexander, and M.C. Reed, "Performance of multicarrier CDMA with iterative detection," Proc. IEEE Int. Conf. Universal Personal Communications, vol.1, pp.131–135, Oct. 1998.
[7] D. Mottier and D. Castelain, "SINR-based channel pre-equalization for uplink multi-carrier CDMA systems," Proc. IEEE Int. Symp. on Personal, Indoor and Mobile Radio Commun. (PIMRC2002), vol.4, pp.1488–1492, Sept. 2002.
[8] S. Kaiser, "Space frequency block coding in the uplink of broadband MC-CDMA mobile radio systems with pre-equalization," Proc. IEEE VTC'03 fall, vol.3, pp.1757–1761, Oct. 2003.
[9] I. Cosovic, M. Schnell, and A. Springer, "On the performance of different channel pre-compensation techniques for uplink time division duplex MC-CDMA," Proc. IEEE VTC'03 fall, vol.2, pp.857–861, Oct. 2003.
[10] T. Lo, "Maximum ratio transmission," IEEE Trans. Commun., vol.47, no.10, pp.1458–1461, Oct. 1999.
[11] K. Caver, "Single-user and multiuser adaptive maximal ratio transmission for Rayleigh channels," IEEE Trans. Veh. Technol., vol.49, no.6, pp.2043–2050, Nov. 2000.
[12] R.T. Derryberry, S.D. Gray, D.M. Ionescu, G. Mandyam, and B. Raghothaman, "Transmit diversity in 3G CDMA systems," IEEE Commun. Mag., vol.33, no.4, pp.68–75, April 2002.
[13] H. Shi, M. Katayama, T. Yamazato, H. Okada, and A. Ogawa, "An adaptive antenna selection scheme for transmit diversity in OFDM systems," Proc. IEEE VTC'01 fall, vol.4, pp.2168–2172, Oct. 2001.
[14] R. Esmailzadeh, M. Nakagawa, and A. Jones, "TDD-CDMA for the 4th generation of wireless communications," IEEE Wirel. Commun., vol.10, no.4, pp.8–15, Aug. 2003.
[15] D. Garg and F. Adachi, "Joint space-time transmit diversity and minimum mean square error equalization for MC-CDMA with antenna diversity reception," IEICE Trans. Commun., vol.E87-B, no.4, pp.849–857, April 2004.
[16] V. Tarokh, H. Jafarkhani, and A.R. Calderbank, "Space-time block coding for wireless communications: Performance results," IEEE J. Sel. Areas Commun., vol.17, no.3, pp.451–460, March 1999.
[17] E.-K. Hong, S.-H. Hwang, K.-J. Kim, and K.-C. Whang, "Synchronous transmission technique for the reverse link in DS-CDMA terrestrial mobile systems," IEEE Trans. Commun., vol.47, no.11, pp.1632–1635, Nov. 1999.

Appendix: Derivation for Variances of MAI and Noise

μ_{MAI} of Eq. (12) can be rewritten as

$$\begin{aligned}\mu_{MAI} &= \sqrt{\frac{2S}{SF}}\frac{1}{SF} \\ &\times \sum_{k=mSF}^{(m+1)SF-1}\sum_{\substack{u=0\\u\neq j}}^{U-1}\begin{Bmatrix}(\tilde{H}_u(k)-\bar{H}_u)\times c_u(k \bmod SF)\\ c_j^*(k \bmod SF)d_u(m)\end{Bmatrix} \\ &+ \sqrt{\frac{2S}{SF}}\frac{1}{SF}\sum_{k=mSF}^{(m+1)SF-1}\sum_{\substack{u=0\\u\neq j}}^{U-1}\bar{H}_u c_u(k \bmod SF) \\ &\times c_j^*(k \bmod SF)d_u(m), \end{aligned} \tag{A·1}$$

where $\bar{H}_u$ is defined as

$$\bar{H}_u = \frac{1}{SF}\sum_{k=mSF}^{(m+1)SF-1}\tilde{H}_u(k). \tag{A·2}$$

Since the spreading sequences $\{c_u(k \bmod SF);\ k = mSF \sim (m+1)SF-1\}$, $u = 0 \sim U-1$, are orthogonal:

$$\sum_{k=mSF}^{(m+1)SF-1} c_u(k)c_j^*(k) = 0, \quad \text{if } u \neq j, \tag{A·3}$$

Eq. (A·1) reduces to

$$\begin{aligned}\mu_{MAI} &= \sqrt{\frac{2S}{SF}}\frac{1}{SF}\sum_{\substack{u=0\\u\neq j}}^{U-1}\sum_{k=mSF}^{(m+1)SF-1}\left(\tilde{H}_u(k)-\bar{H}_u(k)\right) \\ &\times c_u(k)c_j^*(k)d_u(m). \end{aligned} \tag{A·4}$$

Using Eq. (A·4), the variance σ^2_{MAI} of μ_{MAI} can be computed from

$$\begin{aligned}\sigma^2_{MAI} &= \frac{1}{2}E\left[\,|\mu_{MAI}|^2\right] = \frac{S}{SF^3}\sum_{k=mSF}^{(m+1)SF-1}\sum_{k'=mSF}^{(m+1)SF-1} \\ &\times \sum_{\substack{u=0\\u\neq v,j}}^{U-1}\sum_{\substack{v=0\\v\neq u,j}}^{U-1}\begin{Bmatrix}\left(\tilde{H}_u(k)-\bar{H}_u(k)\right)\left(\tilde{H}_v(k')-\bar{H}_v(k')\right)^* \\ \times E\left[c_u(k)c_v^*(k')c_j^*(k)c_j(k')d_u(m)d_v^*(m)\right]\end{Bmatrix}. \end{aligned} \tag{A·5}$$

Since $E\left[d_u(m)d_j^*(m)\right] = 0$ if $u \neq j$, we have

$$\begin{aligned}&\sigma^2_{MAI} \\ &= \frac{S}{SF^3}\sum_{k=mSF}^{(m+1)SF-1}\sum_{k'=mSF}^{(m+1)SF-1}\sum_{\substack{u=0\\u\neq j}}^{U-1}\begin{bmatrix}\left(\tilde{H}_u(k)-\bar{H}_u(k)\right) \\ \times\left(\tilde{H}_u(k')-\bar{H}_u(k')\right)^* \\ \times E\left[c_u(k)c_u^*(k')c_j^*(k)c_j(k')\right]\end{bmatrix} \\ &= \frac{S}{SF}\frac{1}{SF^2}\sum_{k=mSF}^{(m+1)SF-1}\sum_{\substack{u=0\\u\neq j}}^{U-1}\left|\tilde{H}_u(k)-\bar{H}_u(k)\right|^2 \\ &+ \frac{S}{SF^3}\sum_{\substack{k=mSF\\k\neq k'}}^{(m+1)SF-1}\sum_{\substack{k'=mSF\\k\neq k'}}^{(m+1)SF-1}\sum_{\substack{u=0\\u\neq j}}^{U-1}\begin{Bmatrix}\left(\tilde{H}_u(k)-\bar{H}_u(k)\right) \\ \times\left(\tilde{H}_u(k')-\bar{H}_u(k')\right)^* \\ \times E\left[c_u(k)c_u^*(k')c_j^*(k)c_j(k')\right]\end{Bmatrix}, \end{aligned} \tag{A·6}$$

Applying the law of large numbers, the second term becomes zero. Finally, the variance σ^2_{MAI} is given by

$$\sigma^2_{MAI} = \frac{S}{SF}\frac{1}{SF}\sum_{\substack{u=0\\u\neq j}}^{U-1}\left(\frac{1}{SF}\sum_{k=mSF}^{(m+1)SF-1}\left|\tilde{H}_u(k)^2\right| - \left|\frac{1}{SF}\sum_{k=mSF}^{(m+1)SF-1}\tilde{H}_u(k)\right|^2\right). \quad (A\cdot 7)$$

Next, we obtain σ^2_{AWGN}. Using Eq. (12), the variance σ^2_{AWGN} of the noise is obtained from

$$\sigma^2_{AWGN} = \frac{1}{2}\frac{1}{SF^2}\sum_{k=mSF}^{(m+1)SF-1}\sum_{k'=mSF}^{(m+1)SF-1} E\left[n(k)n^*(k')c_j(k)c_j^*(k')\right]. \quad (A\cdot 8)$$

Since $\{n(k); k = mSF \sim (m+1)SF-1\}$ are zero-mean independent complex-valued Gaussian variables having a variance of $2N_0/N_cT_c$, we have

$$\sigma^2_{AWGN} = \frac{1}{SF}\frac{N_0}{N_cT_c}. \quad (A\cdot 9)$$

Hiromichi Tomeba received his B.S. degree in communications engineering from Tohoku University, Sendai, Japan, in 2004. Currently he is a graduate student at the Department of Electrical and Communications Engineering, Graduate School of Engineering, Tohoku University. His research interests include frequency-domain pre-equalization and antenna diversity techniques for mobile communication systems.

Shinsuke Takaoka received his B.S. and M.S. degree in communications engineering from Tohoku University, Sendai, Japan, in 2001 and 2003. Currently, he is a graduate student at the Department of Electrical and Communications Engineering, Tohoku University. His research interests include digital signal transmission techniques, especially for mobile communication systems.

Fumiyuki Adachi See this issue, p.499.